Aquaporin-4 and GPRC5B: old and new players in controlling brain oedema

Emma M. J. Passchier,[1,2,†] Sven Kerst,[1,2,†] Eelke Brouwers,[1,2,†] Eline M. C. Hamilton,[1,†] Quinty Bisseling,[1,2] Marianna Bugiani,[3] Quinten Waisfisz,[4] Philip Kitchen,[5] Lucas Unger,[5] Marjolein Breur,[1,3] Leoni Hoogterp,[1] Sharon I. de Vries,[6] Truus E. M. Abbink,[1] Maarten H. P. Kole,[6,7] Rob Leurs,[8] Henry F. Vischer,[8] Maria S. Brignone,[9] Elena Ambrosini,[9] François Feillet,[10] Alfred P. Born,[11] Leon G. Epstein,[12] Huibert D. Mansvelder,[2] Rogier Min[1,2,‡] and Marjo S. van der Knaap[1,2,‡]

[†,‡]**These authors contributed equally to this work.**

Abstract

Brain oedema is a life-threatening complication of various neurological conditions. Understanding molecular mechanisms of brain volume regulation is critical for therapy development. Unique insight comes from monogenic diseases characterized by chronic brain oedema, of which megalencephalic leukoencephalopathy with subcortical cysts (MLC) is the prototype. Variants in *MLC1* or *GLIALCAM*, encoding proteins involved in astrocyte volume regulation, are the main causes of MLC. In some patients the genetic cause remains unknown.

We performed genetic studies to identify novel gene variants in MLC patients, diagnosed by clinical and MRI features, without *MLC1* or *GLIALCAM* variants. We determined subcellular localization of the related novel proteins in cells and in human brain tissue. We investigated functional consequences of the newly identified variants on volume regulation pathways using cell volume measurements, biochemical analysis and electrophysiology.

We identified a novel homozygous variant in *AQP4*, encoding the water channel aquaporin-4, in two siblings, and two *de novo* heterozygous variants in *GPRC5B*, encoding the orphan G protein-coupled receptor GPRC5B, in three unrelated patients. The *AQP4* variant disrupts membrane localization and thereby channel function. GPRC5B, like MLC1, GlialCAM and aquaporin-4, is expressed in astrocyte endfeet in human brain. Cell volume regulation is disrupted in GPRC5B

patient-derived lymphoblasts. GPRC5B functionally interacts with ion channels involved in astrocyte volume regulation.

In conclusion, we identify aquaporin-4 and GPRC5B as old and new players in genetic brain oedema. Our findings shed light on the protein complex involved in astrocyte volume regulation and identify GPRC5B as novel potentially druggable target for treating brain oedema.

Author affiliations:

1 Department of Child Neurology, Amsterdam Leukodystrophy Center, Emma Children's Hospital, Amsterdam University Medical Centers, location Vrije Universiteit Amsterdam, Amsterdam Neuroscience, Amsterdam, The Netherlands

2 Department of Integrative Neurophysiology, Center for Neurogenomics and Cognitive Research, Vrije Universiteit Amsterdam, Amsterdam Neuroscience, Amsterdam, The Netherlands

3 Department of Pathology, Amsterdam Leukodystrophy Center, Amsterdam University Medical Centers, location Vrije Universiteit Amsterdam, Amsterdam Neuroscience, Amsterdam, The Netherlands

4 Department of Human Genetics, Amsterdam University Medical Centers location Vrije Universiteit Amsterdam, Amsterdam, The Netherlands

5 School of Biosciences, College of Health and Life Sciences, Aston University, Birmingham, UK

6 Department of Axonal Signaling, Netherlands Institute for Neuroscience, Royal Netherlands Academy of Arts and Sciences, Amsterdam, The Netherlands

7 Cell Biology, Neurobiology and Biophysics, Department of Biology, Faculty of Science, Utrecht University, Utrecht, The Netherlands

8 Division of Medicinal Chemistry, Faculty of Science, Amsterdam Institute of Molecular and Life Sciences, Vrije Universiteit Amsterdam, Amsterdam, The Netherlands

9 Department of Neuroscience, Istituto Superiore di Sanità, Rome, Italy

10 Reference Center for Inherited Metabolic Diseases, INSERM UMR_S 1256 NGERE, Nancy University Hospital, Vandoeuvre-lès-Nancy, France

11 Department of Pediatrics and Adolescent Medicine, Rigshospitalet, Copenhagen University Hospital, Copenhagen, Denmark

12 Division of Neurology, Ann & Robert H. Lurie Children's Hospital of Chicago, Chicago, Illinois; Departments of Pediatrics and Neurology, Northwestern University Feinberg School of Medicine, Chicago, Illinois

Correspondence to: Marjo van der Knaap

Amsterdam UMC

Meibergdreef 9

1105 AZ Amsterdam, The Netherlands

E-mail: ms.vanderknaap@amsterdamumc.nl

Correspondence may also be addressed to: Rogier Min

E-mail: r.min@amsterdamumc.nl

Running title: AQP4 and GPRC5B in genetic brain oedema

Keywords: leukodystrophy; brain oedema; aquaporin-4; GPRC5B; volume regulation

Abbreviations: AQP = aquaporin; GPCR = G protein-coupled receptor; MLC = megalencephalic leukoencephalopathy with subcortical cysts; RVD = regulatory volume decrease; SNP = single nucleotide polymorphism; VRAC = volume regulated anion channel; WES = whole exome sequencing

Introduction

All cells in the body have systems to sense and correct volume changes.[1] Volume regulation is especially critical in the brain, encased by a rigid skull. While other organs tolerate marked volume changes, brain swelling soon leads to potentially lethal herniation. Brain oedema is a much-feared complication of trauma, infection, tumour and infarction.[2] Hyperventilation, infusion of hypertonic solutions and craniectomy are moderately effective measures to combat brain oedema, but mortality remains high and permanent neurological deficits common.[3] Identifying molecular players involved in brain volume regulation is critical in the search for new approaches to target brain oedema.

Neuronal activity places extra strain on brain volume regulation. It is mediated by shifts in ions and neurotransmitters, which are accompanied by osmotically driven shifts in water.[4] Strict volume sensing and tightly regulated compensatory mechanisms guarantee rapid correction, thus preventing large changes in volume and maintaining ionic and neurotransmitter homeostasis essential for proper neurophysiological function.[5,6] Glial cells, especially astrocytes, are central in brain volume regulation. Astrocytes form a syncytium with interconnected oligodendrocytes and ependymal cells that is critical for long-distance dispersion and disposal of ions and water and for buffering associated volume changes. The importance of such systems is illustrated by conditions with massive neural firing, such as status epilepticus, which may overwhelm compensatory mechanisms and lead to life threatening brain oedema.

Molecular mechanisms of cellular volume sensing and regulation have been deciphered in part. Aquaporins (AQPs), a large family of membrane water channels, have emerged as crucial components.[7] In the brain, aquaporin-4 (AQP4), encoded by the gene *AQP4*, is the most prevalent. It is present in very high density in astrocyte endfeet at blood-brain and cerebrospinal fluid-brain interfaces. Despite the well-established importance of AQP4 in brain volume regulation, no monogenic human disease has been associated with pathogenic variants in *AQP4*.

Studies of monogenic diseases characterized by brain oedema have contributed molecular insights in brain volume regulating pathways. Of these, megalencephalic leukoencephalopathy with subcortical cysts (MLC), displaying chronic white matter oedema, is the prototype. In 98% of cases, pathogenic variants in *MLC1* or *GLIALCAM* are found, both causing loss of MLC1

function. MLC1 is a membrane protein almost exclusively expressed in astrocyte endfeet, a location shared with AQP4 and other proteins involved in ion and water homeostasis. Loss of MLC1 function leads to partial loss of volume-regulated anion channel (VRAC) function and slowing of the regulatory volume decrease (RVD) after cell swelling. Other monogenic diseases characterized by brain oedema are leukoencephalopathies caused by recessive variants in *CLCN2* and *GJB1*, encoding chloride channel ClC-2 and gap-junction protein connexin32, respectively.[6,8]

In approximately 2% of MLC patients, no pathogenic variants in *MLC1* or *GLIALCAM* are found. Among these patients, we discovered variants in two genes: *AQP4* and *GPRC5B*. *GPRC5B* encodes G protein-coupled receptor class C group 5 member B (GPRC5B), an orphan G protein-coupled receptor (GPCR) of unknown function, recently implicated in astrocyte volume regulation.[9] We experimentally substantiate the functional relevance of the newly identified gene variants.

Materials and methods

Detailed materials and methods are available at *Brain* online. A summary is presented below.

Study oversight

With approval of the Institutional Review Board, we performed genetic studies in patients with an MRI-based diagnosis of MLC and no pathogenic variants in *MLC1* and *GLIALCAM*. Written informed consent was obtained from the families. Referring physicians provided clinical characteristics.[10]

Genetic analysis

We performed whole exome sequencing (WES) on genomic DNA from three unrelated patients (patients 1-3). For one patient parental DNA was included to form a family trio. Data was analysed as described. Patients 4 and 5, siblings with consanguineous parents, lacked possible pathogenic variants in the gene identified in patients 1-3. We executed single nucleotide polymorphism (SNP) array analysis to identify runs of homozygosity larger than 1 Mb and

overlapping regions. Validation and segregation of the identified gene variants were performed by Sanger sequencing.

Cellular and molecular studies

HEK293T cells, Madine-Darby Canine Kidney (MDCK) cells, lymphoblasts and U251 astrocytoma cells were maintained as described.[11-13] Stably AQP4-transfected MDCK cells and HEK293T cells transiently transfected with AQP4 were used for confocal imaging of AQP4 expression, cell surface biotinylation experiments, western blots and calcein-quenching measurements of cell volume changes.[14] Lymphoblasts were used for measuring RVD[12] and for western blot experiments.[11] GPRC5B-transfected U251 cells were used for whole cell patch-clamp analysis.

Immunohistochemistry and electron microscopy

Localization of GPRC5B in the human brain was studied in frontal lobe tissue obtained at autopsy from four control subjects of different ages. Tissue processing and microscopy was performed as described.[8]

Statistics

Comparisons were made using Student's t-test (nested where appropriate), Mann-Whitney test or Kruskal-Wallis test. Statistically significant differences were defined as $P \leq 0.05$. Data are represented as mean ± SEM.

Data availability

Data is available upon reasonable request.

Results

GPRC5B and *AQP4* variants

Genetic studies were performed in five patients with an MRI-based diagnosis of MLC and no pathogenic variants in *MLC1* or *GLIALCAM*. Family trio analysis of patient 1 yielded several

candidate variants; comparison with patients 2 and 3 revealed *GPRC5B* as only candidate with a heterozygous variant in all three patients. Two different exonic duplications were identified in transcript NM_016235.2: c.526_528dup, p.(Ile176dup) in patients 1 and 2, c.528_530dup, p.(Ala177dup) in patient 3. Both encoded amino acids are located in the fourth transmembrane protein domain. The variants were absent in parents, suggesting they arose *de novo*. An unaffected sibling did not harbour the variant. These variants are not present in gnomAD (v2.1.1; gnomad.broadinstitute.org). Sharing the gene on GeneMatcher[15] did not reveal additional patients. *GPRC5B* encodes GPRC5B belonging to the group of metabotropic glutamate receptor-like proteins.[16] Variants in *GPRC5B* have so far not been associated with disease.

In sibling patients 4 and 5, with consanguineous parents, we did not find variants in *GPRC5B.* SNP-array revealed six runs of homozygosity larger than 1 Mb with overlapping regions. Screening of genes in these regions identified *AQP4* as most promising candidate. Sanger sequencing revealed a c.643G>A, p.(Ala215Thr) variant in transcript NM_001650.5, homozygous in both patients and heterozygous in parents. This variant has been reported (rs148498248) in a few heterozygous carriers in gnomAD (v2.1.1 in 4 out of 251462 alleles), but not homozygous. GeneMatcher[15] again did not reveal additional patients. The change concerns a highly conserved nucleotide and amino acid (phyloP: 5.94 [-14.1;6.4]). The variant is predicted to be deleterious (Polyphen-2 score 0.998, Align-GVGD (v2007): C55 [GV: 0.00 - GD: 58.02], and SIFT score 0). Ala215 is part of the highly conserved Asparagine-Proline-Alanine (NPA) motif in the M7 loop of AQP4.[17]

Clinical and MRI phenotype

Clinical details and use of antiepileptic drugs are summarized in Supplementary Table 1.

The patients with heterozygous *GPRC5B* variants (patients 1-3), had healthy, non-consanguineous parents and no affected siblings. All developed macrocephaly in the first year of life and remained macrocephalic. Patients 1 and 2, both male, had delayed motor development. Patient 1 never walked without support. Early-onset slow motor decline was characterized by spasticity, ataxia and variable dystonia. Both became fully wheelchair-dependent at age 6 years. Patient 1 developed severe epilepsy from age 4 years; patient 2 had mild epilepsy from 14 years. Slow cognitive decline occurred. At 19 years, patient 1 had limited motor function, marked cognitive deficit, and no speech. At 27 years, patient 2 was still able to handle objects and

operate an electric wheelchair. His speech had deteriorated. Patient 3, a female, had normal early motor and cognitive development. From age 8 years, progressive ataxia and spasticity developed; she became fully wheelchair dependent at 12 years. At 24 years, she had mild cognitive deficit and mood problems. She experienced a few epileptic seizures.

Patients 1-3 underwent 7 MRIs between 6 months and 11 years. All MRIs showed the same picture of classic, unremitting MLC[18] with diffusely abnormal and swollen cerebral white matter and subcortical cysts in the anterior temporal and frontal white matter without improvement after the age of 2 years. Figure 1 illustrates the MRI of patient 3 at 11 years of age, as compared to age-matched normal MRI (Fig. 1A-C).

The patients with the homozygous *AQP4* variant (patients 4 and 5), male and female, were the only children of healthy parents, who had a normal head circumference. Both patients developed macrocephaly in the first 6 months of life; head circumference normalized in the boy and remained just above 2 SD in the girl. Both displayed developmental delay and hypotonia, with unsupported walking from ages 5 and 2 years, respectively. Both had epilepsy from age 1 year. The boy initially had frequent status epilepticus; his epilepsy came under control with multiple anti-epileptic drugs. In the girl, epilepsy was well controlled with medication. At 16 years, the boy had marked cognitive deficit with limited language ability and behavioural problems. He could walk without support with difficulty and had limited hand function. At 13 years, the girl had close to normal motor function and mild cognitive deficit.

Patient 4 had the first MRI at 8 months, which showed diffuse signal abnormality and mild swelling of the cerebral white matter and subcortical cysts in the anterior temporal region, consistent with MLC (Fig. 1A,D,E). Follow-up MRI at 4 years showed normalization of the cerebral white matter, but persistence of small anterior temporal cysts (Fig. 1B,E). The MRI of patient 5 at 7 months of age showed the same picture, but somewhat milder. The MRI pattern is similar to remitting MLC.[18]

Effects of variants on AQP4 localization and function

MDCK cells are well suited for assessment of AQP4-mediated water transport because of their low basal water permeability.[13] MDCK lines with stable expression of the M1 isoform of either wild-type AQP4 or Ala215Thr AQP4 (Fig. 2A), fused to a C-terminal green-fluorescent-protein

(GFP) tag, were generated.[13] Western blot analysis revealed clear expression of wild-type AQP4 protein, but no detectable expression of Ala215Thr AQP4 (Fig. 2B), suggesting that the mutant protein is unstable, potentially due to misfolding, and therefore rapidly degraded. In line with this, cell surface biotinylation followed by ELISA revealed no membrane expression of Ala215Thr AQP4, while wild-type AQP4 was clearly detectable (Fig. 2C). To assess AQP4 function, cells expressing wild-type or Ala215Thr AQP4 were exposed to a hypotonic or hypertonic shock, inducing cell swelling or shrinking, respectively. While swelling and shrinking rate constants were clearly increased in a stable wild-type AQP4 MDCK line, rate constants were indistinguishable from non-transfected MDCK cells for the Ala215Thr AQP4 lines (Fig. 2D-G).

We performed transient overexpression studies in HEK293T cells. Cells were transiently transfected with GFP tagged AQP4 plasmids, which leads to exclusive expression of the M1 AQP4 isoform.[19] Confocal imaging revealed membrane localization for wild-type AQP4, which was strongly reduced for the Ala215Thr variant (Fig. 3A-C). Ala215Thr AQP4 was detectable in transfected HEK293T cells using SDS-page followed by western blot, but while wild-type AQP4 was mainly detected as monomer and dimer, Ala215Thr AQP4 formed large protein aggregates (Fig. 3D), suggesting misfolding and intracellular retention of the mutant protein. The difference with stable MDCK cells, which lacked detectable Ala215Thr AQP4, might be explained by the massive protein overexpression upon transient transfection in HEK293T cells saturating protein degradation pathways. Cell surface biotinylation experiments of transfected HEK293T cells followed by ELISA revealed a ~60% reduction in membrane localization of Ala215Thr AQP4 compared to wild-type (Fig. 3E). To assess function of the remaining AQP4 protein, transfected HEK293T cells were exposed to a hypotonic or hypertonic shock, inducing cell swelling or shrinking, respectively. Overexpression of wild-type AQP4 led to fast swelling and shrinking, visible when normalizing to non-transfected cells (Fig. 3F). Ala215Thr AQP4 overexpression still increased swelling and shrinking compared to non-transfected cells, but the rates were significantly reduced in comparison to wild-type AQP4 (Fig. 3G), suggesting that the Ala215Thr AQP4 reaching the cell membrane retains some water channel function. Further quantitative assessment of the functionality of the remaining membrane Ala215Thr AQP4 is hampered by the fact that HEK293T cells are not well suited for water permeability assays due to low adherence, which causes artefacts.

GPRC5B localization in human brain

In mouse brain, a proportion of GPRC5B localizes with MLC1 in perivascular domains.[9] Its localization in human brain is unknown. Immunofluorescence microscopy on human brain tissue revealed staining of GPRC5B in astrocyte cell bodies in white matter, in addition to clear perivascular staining (Fig. 4A,B), which was surrounded by and partially overlapping with GlialCAM staining (Fig. 4C). GPRC5B was also detected in the glia limitans and in ependymal cells, but not in neurons (Fig. 4D-F). mRNA and protein levels of GPRC5B in the human brain increased with age, similar to MLC1[20] (Supplementary Fig. 1).

Immunogold labelling of GPRC5B followed by electron microscopy (Fig. 4G) revealed membranous labelling in the perivascular region in astrocyte endfeet, confirming proximity of GPRC5B to MLC1, GlialCAM, AQP4 and other proteins involved in astrocyte ion and water homeostasis. Membranous labelling was also observed in endothelial cells and pericytes. Lymphocytes showed intracellular and membranous GPRC5B labelling.

Effects of *GPRC5B* variants on cell physiology

We investigated the impact of *GPRC5B* variants on cell physiology in patient lymphoblasts. Lymphoblasts from MLC patients with biallelic *MLC1* variants display disrupted RVD following swelling induced by hypotonic shock.[12] Recording RVD in lymphoblasts from patients 1-3 and five controls (Fig. 5A-C) showed that RVD was also reduced in cells from patients with *GPRC5B* variants. Western blot analysis revealed a strong increase in GPRC5B levels in patient lymphoblasts compared to controls (Fig. 5D,E). Reducing GPRC5B expression in mouse primary astrocytes reduces MLC1 levels,[9] but the increased GPRC5B levels in patient cells were not accompanied by altered MLC1 levels (Fig. 5E). AQP4 and the crucial VRAC-subunit LRRC8A were not detected in lymphoblasts from patients or controls with western blot. The swelling-activated cation-channel TRPV4 was strongly downregulated (Fig. 5E). Together, these findings indicate disturbed volume regulation in lymphoblasts from patients with *GPRC5B* variants, potentially due to increased GPRC5B levels.

Disrupted activation of VRACs is a key feature of MLC,[12,21] and recently GPRC5B knockdown in astrocytes has been shown to hamper VRAC activity.[9] We performed whole-cell patch clamp recordings of transfected human U251 astrocytoma cells to study VRAC activity. MLC1

overexpression in multiple cell types, including U251 cells, increases VRAC activity.[12,22] Similarly, GPRC5B overexpression increased VRAC activity (Fig. 5F-H). Remarkably, wild-type, Ile176dup and Ala177dup GPRC5B were equally effective in increasing VRAC currents (Fig. 5G,H). Alternative splicing can result in an N-terminally extended GPRC5B isoform (isoform 2). Expression of wild-type or patient variants of isoform 2 led to a similar increase in VRAC currents as observed for isoform 1 (Fig. 5H). To investigate a potential interaction between MLC1 and GPRC5B, U251 cells stably expressing recombinant MLC1[11] were transfected with plasmids expressing wild-type GPRC5B or the patient variants. Under these conditions, GPRC5B did not have an additive effect on VRAC activity over MLC1 overexpression (Fig. 5I), suggesting that MLC1 and GPRC5B modulate VRAC currents through a common pathway.

Discussion

We explore new genetic causes of brain white matter oedema and describe novel pathogenic variants in AQP4 and GPRC5B leading to chronic white matter oedema with the phenotype of MLC. Our results provide the first description of how defective AQP4 affects the human brain. That a defect in AQP4 leads to disturbed brain water homeostasis is as expected, but it is surprising that the resulting white matter oedema is remitting. Similarly, heterozygous defects in a specific GlialCAM domain cause MLC with infantile-onset oedema that resolves in a few years.[23] The white matter oedema associated with the described GPRC5B variants is unremitting and indistinguishable from that caused by bi-allelic loss of function defects in MLC1 or GlialCAM. GPRC5B and AQP4 share their localization in astrocyte endfeet with MLC1, GlialCAM, ClC-2 and several other proteins involved in ion and water homeostasis.[6] Our findings confirm the crucial role of the astrocyte endfoot volume regulating protein complex in controlling brain oedema. Defects in ion and water homeostasis are associated with increased risk of epilepsy,[24] also in patients with AQP4 and GPRC5B defects.

Despite the critical physiological function of AQPs, very few diseases have been linked to AQP genetic defects. Biallelic *AQP1* variants impair the ability to concentrate urine.Recessive[25] and dominant[26] *AQP2* variants cause nephrogenic diabetes insipidus. Diseases

unequivocally related to pathogenic *AQP4* variants have not been described.[27] The variant reported here, Ala215Thr, affects the second NPA motif of AQP4. Almost all AQP family members contain these two highly conserved NPA motifs, forming the narrow central part of the water channel, crucial for selective water permeability[7] and plasma membrane localization. Indeed, our results indicate that the Ala215Thr variant abolishes AQP4 (membrane) expression in a stable cell line, probably because the protein is misfolded and rapidly degraded. Upon strong overexpression the mutant protein is detectable, but mostly forms aggregates. Under these conditions cellular degradation pathways are probably saturated and unable to degrade all mutant protein, and some of the remaining protein reaches the membrane. This remaining protein has some water channel functionality, but the physiological relevance of this is unclear.

GPCRs enable cells to respond to chemical messengers, protein-protein interactions and mechanical force, such as swelling. The ligand of GPRC5B has not been identified. Recently, GPRC5B was identified as interacting partner of MLC1 and GlialCAM.[9] Our findings confirm that GPRC5B, like MLC1, modulates VRAC activity.[12] Loss of MLC1 function reduces VRAC activity, while MLC1 overexpression increases it.[12] Similarly, knockdown of GPRC5B reduces VRAC activity[9] and we show that GPRC5B overexpression increases it. Loss of MLC1 function causes MLC,[18,20] but MLC1 overexpression in mice also leads to an MLC phenotype,[28] highlighting the critical importance of fine-tuned volume regulation by astrocytes. The variants Ile176dup and Ala177dup are associated with highly increased GPRC5B expression levels in patient cells, and the effect of Ile176dup or Ala177dup GPRC5B overexpression on VRAC activity is indistinguishable from wild-type GPRC5B overexpression. It is therefore likely that increased GPRC5B expression causes chronic white matter oedema by disrupting fine-tuning of the essential volume-regulating channels VRAC and TRPV4.[11] This could explain how heterozygous variants are sufficient to cause a full-blown MLC phenotype.

Several anti-epileptic drugs have been suggested to inhibit AQP4 function[29], although these effects have not been reproduced by others[30]. Our patients were treated with anti-epileptic drugs in various combinations at different times (see Supplementary Table 1). Overall, we did not observe a consistent differential effect of the different drugs on epilepsy control or the neurological picture outside the epilepsy. Worsening of seizures in the AQP4 patients was not observed with any of the drugs.

Insight into the molecular components of volume regulating pathways is conditional for finding targets to combat brain oedema in critical conditions, like stroke and trauma. Deciphering genetic defects causing brain oedema provides valuable information on compensatory routes preventing oedema under normal conditions. AQP4 is considered a promising therapeutic target for treatment of brain oedema, and drugs that target permeability or localization[31] of AQP4 are being developed. It is notable that white matter oedema in our patients with reduced AQP4 function resolves spontaneously, which could be related to residual activity but could also suggest redundancy in related ion and water compensatory pathways. By contrast, white matter oedema is not remitting in patients with *GPRC5B* variants. GPCRs are exceptionally suited as drug target. We suggest that targeting GPRC5B signalling might constitute a new strategy for treatment of brain oedema.

Intriguingly, other pathologies have been associated with proteins involved in brain volume regulation. Auto-immunity against AQP4 causes neuromyelitis optica, while antibodies provoked by Epstein–Barr virus infection and cross-reacting with GlialCAM are associated with multiple sclerosis.[32] Genome-wide association studies link GPRC5B to obesity.[33] Adipocytes dramatically swell upon fat accumulation, and adipocyte and astrocyte volume regulation show key similarities. GPRC5B signalling impacts cardiovascular health,[34] insulin secretion and diabetes.[35,36] Therefore, understanding roles of proteins in volume regulation and identifying modulators may impact major healthcare challenges other than brain oedema.

Acknowledgements

We thank the patients and families for their participation in the study; N. Postma, T.J. ter Braak, C. van Berkel and G.M. van Leeuwen (Amsterdam UMC), and J.C. Lodder (Vrije Universiteit Amsterdam) for excellent technical assistance; R. Zalm and X. Ma (Vrije Universiteit Amsterdam) for assistance with cloning; A.C. Conner (University of Birmingham, UK) for providing the wild-type AQP4-GFP construct.

Funding

Supported in part by grants from ZonMW (VIDI grant 91718392) and the Dutch Rare Disease Foundation (Zeldzame Ziekten Fonds). TEMA, RM and MvdK are members of the European reference network for rare neurological disorders (ERN-RND), project ID 739510.

Competing interests

The authors report no competing interests.

Supplementary material

Supplementary material is available at *Brain* online.

References

1. Hoffmann EK, Lambert IH, Pedersen SF. Physiology of cell volume regulation in vertebrates. *Physiol Rev*. Jan 2009;89(1):193-277. doi:10.1152/physrev.00037.2007

2. Fishman RA. Brain edema. *N Engl J Med*. Oct 2 1975;293(14):706-11. doi:10.1056/NEJM197510022931407

3. Marmarou A. A review of progress in understanding the pathophysiology and treatment of brain edema. *Neurosurg Focus*. May 15 2007;22(5):E1. doi:10.3171/foc.2007.22.5.2

4. Somjen GG. Ion regulation in the brain: implications for pathophysiology. *Neuroscientist*. Jun 2002;8(3):254-67. doi:10.1177/1073858402008003011

5. Rash JE. Molecular disruptions of the panglial syncytium block potassium siphoning and axonal saltatory conduction: pertinence to neuromyelitis optica and other demyelinating diseases of the central nervous system. *Neuroscience*. 7/28/2010 2010;168(4):982-1008. Not in File. doi:S0306-4522(09)01712-6 [pii];10.1016/j.neuroscience.2009.10.028 [doi]

6. Min R, Van der Knaap MS. Genetic defects disrupting glial ion and water homeostasis in the brain. *Brain Pathol*. May 2018;28(3):372-387. doi:10.1111/bpa.12602

7. King LS, Kozono D, Agre P. From structure to disease: the evolving tale of aquaporin biology. *Nat Rev Mol Cell Biol*. Sep 2004;5(9):687-98. doi:10.1038/nrm1469

8. Depienne C, Bugiani M, Dupuits C, *et al*. Brain white matter oedema due to ClC-2 chloride channel deficiency: an observational analytical study. *Lancet Neurol*. Jul 2013;12(7):659-68. doi:10.1016/S1474-4422(13)70053-X

9. Alonso-Gardon M, Elorza-Vidal X, Castellanos A, *et al*. Identification of the GlialCAM interactome: the G protein-coupled receptors GPRC5B and GPR37L1 modulate megalencephalic leukoencephalopathy proteins. *Hum Mol Genet*. Aug 12 2021;30(17):1649-1665. doi:10.1093/hmg/ddab155

10. Hamilton EMC, Tekturk P, Cialdella F, *et al*. Megalencephalic leukoencephalopathy with subcortical cysts: Characterization of disease variants. *Neurology*. Apr 17 2018;90(16):e1395-e1403. doi:10.1212/WNL.0000000000005334

11. Lanciotti A, Brignone MS, Molinari P, *et al*. Megalencephalic leukoencephalopathy with subcortical cysts protein 1 functionally cooperates with the TRPV4 cation channel to activate the response of astrocytes to osmotic stress: dysregulation by pathological mutations. *Hum Mol Genet*. 5/15/2012 2012;21(10):2166-2180. Not in File. doi:dds032 [pii];10.1093/hmg/dds032 [doi]

12. Ridder MC, Boor I, Lodder JC, *et al*. Megalencephalic leucoencephalopathy with cysts: defect in chloride currents and cell volume regulation. *Brain*. 11/2011 2011;134(Pt 11):3342-3354. Not in File. doi:awr255 [pii];10.1093/brain/awr255 [doi]

13. Kitchen P, Conner AC. Control of the Aquaporin-4 Channel Water Permeability by Structural Dynamics of Aromatic/Arginine Selectivity Filter Residues. *Biochemistry*. Nov 17 2015;54(45):6753-5. doi:10.1021/acs.biochem.5b01053

14. Kitchen P, Salman MM, Abir-Awan M, *et al*. Calcein Fluorescence Quenching to Measure Plasma Membrane Water Flux in Live Mammalian Cells. *STAR Protoc*. Dec 18 2020;1(3):100157. doi:10.1016/j.xpro.2020.100157

15. Sobreira N, Schiettecatte F, Valle D, Hamosh A. GeneMatcher: a matching tool for connecting investigators with an interest in the same gene. *Hum Mutat*. Oct 2015;36(10):928-30. doi:10.1002/humu.22844

16. Brauner-Osborne H, Krogsgaard-Larsen P. Sequence and expression pattern of a novel human orphan G-protein-coupled receptor, GPRC5B, a family C receptor with a short amino-terminal domain. *Genomics*. Apr 15 2000;65(2):121-8. doi:10.1006/geno.2000.6164

17. Nagelhus EA, Ottersen OP. Physiological roles of aquaporin-4 in brain. *Physiol Rev*. Oct 2013;93(4):1543-62. doi:10.1152/physrev.00011.2013

18. Van der Knaap MS, Boor I, Estevez R. Megalencephalic leukoencephalopathy with subcortical cysts: chronic white matter oedema due to a defect in brain ion and water homoeostasis. *Lancet Neurol*. 11/2012 2012;11(11):973-985. Not in File. doi:S1474-4422(12)70192-8 [pii];10.1016/S1474-4422(12)70192-8 [doi]

19. Kitchen P, Day RE, Taylor LH, *et al*. Identification and Molecular Mechanisms of the Rapid Tonicity-induced Relocalization of the Aquaporin 4 Channel. *J Biol Chem*. Jul 3 2015;290(27):16873-81. doi:10.1074/jbc.M115.646034

20. Dubey M, Bugiani M, Ridder MC, *et al*. Mice with megalencephalic leukoencephalopathy with cysts: a developmental angle. *Ann Neurol*. 1/2015 2015;77(1):114-131. Not in File. doi:10.1002/ana.24307 [doi]

21. Elorza-Vidal X, Sirisi S, Gaitan-Penas H, *et al*. GlialCAM/MLC1 modulates LRRC8/VRAC currents in an indirect manner: Implications for megalencephalic leukoencephalopathy. *Neurobiol Dis*. Nov 2018;119:88-99. doi:10.1016/j.nbd.2018.07.031

22. Brignone MS, Lanciotti A, Michelucci A, *et al*. MLC1: A New Calcium-regulated Protein Conferring Calcium Dependence to Volume-regulated Anion Channels (VRAC) in Astrocytes. *ResearchSquare*. 2022/03/02 2022;doi:10.21203/rs.3.rs-1195518/v1

23. Lopez-Hernandez T, Ridder MC, Montolio M, *et al*. Mutant GlialCAM causes megalencephalic leukoencephalopathy with subcortical cysts, benign familial macrocephaly, and macrocephaly with retardation and autism. *Am J Hum Genet*. 4/8/2011 2011;88(4):422-432. Not in File. doi:S0002-9297(11)00057-7 [pii];10.1016/j.ajhg.2011.02.009 [doi]

24. Dubey M, Brouwers E, Hamilton EMC, *et al*. Seizures and disturbed brain potassium dynamics in the leukodystrophy megalencephalic leukoencephalopathy with subcortical cysts. *Ann Neurol*. Mar 2018;83(3):636-649. doi:10.1002/ana.25190

25. Deen PM, Verdijk MA, Knoers NV, *et al*. Requirement of human renal water channel aquaporin-2 for vasopressin-dependent concentration of urine. *Science*. Apr 1 1994;264(5155):92-5. doi:10.1126/science.8140421

26. Kuwahara M, Iwai K, Ooeda T, *et al*. Three families with autosomal dominant nephrogenic diabetes insipidus caused by aquaporin-2 mutations in the C-terminus. *Am J Hum Genet*. Oct 2001;69(4):738-48. doi:10.1086/323643

27. Berland S, Toft-Bertelsen TL, Aukrust I, *et al*. A de novo Ser111Thr variant in aquaporin-4 in a patient with intellectual disability, transient signs of brain ischemia, transient cardiac hypertrophy, and progressive gait disturbance. *Cold Spring Harb Mol Case Stud*. Feb 2018;4(1)doi:10.1101/mcs.a002303

28. Sugio S, Tohyama K, Oku S, *et al*. Astrocyte-mediated infantile-onset leukoencephalopathy mouse model. *Glia*. Jan 2017;65(1):150-168. doi:10.1002/glia.23084

29. Huber VJ, Tsujita M, Kwee IL, Nakada T. Inhibition of aquaporin 4 by antiepileptic drugs. *Bioorg Med Chem*. Jan 1 2009;17(1):418-24. doi:10.1016/j.bmc.2007.12.038

30. Yang B, Zhang H, Verkman AS. Lack of aquaporin-4 water transport inhibition by antiepileptics and arylsulfonamides. *Bioorg Med Chem*. Aug 1 2008;16(15):7489-93. doi:10.1016/j.bmc.2008.06.005

31. Kitchen P, Salman MM, Halsey AM, *et al*. Targeting Aquaporin-4 Subcellular Localization to Treat Central Nervous System Edema. *Cell*. May 14 2020;181(4):784-799 e19. doi:10.1016/j.cell.2020.03.037

32. Lanz TV, Brewer RC, Ho PP, *et al*. Clonally expanded B cells in multiple sclerosis bind EBV EBNA1 and GlialCAM. *Nature*. Mar 2022;603(7900):321-327. doi:10.1038/s41586-022-04432-7

33. Speliotes EK, Willer CJ, Berndt SI, *et al*. Association analyses of 249,796 individuals reveal 18 new loci associated with body mass index. *Nat Genet*. Nov 2010;42(11):937-48. doi:10.1038/ng.686

34. Carvalho J, Chennupati R, Li R, *et al*. Orphan G Protein-Coupled Receptor GPRC5B Controls Smooth Muscle Contractility and Differentiation by Inhibiting Prostacyclin Receptor Signaling. *Circulation*. Apr 7 2020;141(14):1168-1183. doi:10.1161/CIRCULATIONAHA.119.043703

35. Kim YJ, Greimel P, Hirabayashi Y. GPRC5B-Mediated Sphingomyelin Synthase 2 Phosphorylation Plays a Critical Role in Insulin Resistance. *iScience*. Oct 26 2018;8:250-266. doi:10.1016/j.isci.2018.10.001

36. Soni A, Amisten S, Rorsman P, Salehi A. GPRC5B a putative glutamate-receptor candidate is negative modulator of insulin secretion. *Biochem Biophys Res Commun*. Nov 22 2013;441(3):643-8.

37. Jung JS, Preston GM, Smith BL, Guggino WB, Agre P. Molecular structure of the water channel through aquaporin CHIP. The hourglass model. *J Biol Chem*. May 20 1994;269(20):14648-54.

Figure legends

Figure 1 Brain MRI in patients with pathogenic *GPRC5B* or *AQP4* variants and age-matched individuals with normal MRI. In all persons, on the left a sagittal T1-weighted image through the temporal lobe is presented, in the middle an axial FLAIR image through the temporal lobe, and on the right an axial T2-weighted image at the level of the lateral ventricles. The first row (A) shows the normal MRI at age 8 months. Compared to the cortex, the partially myelinated white matter is mildly hyperintense on the T1-weighted image (left) and isointense or mildly hypointense on the T2-weighted image (right). There are no temporal subcortical cysts. The second row (B) shows the normal MRI at age 6 years. Compared to the cortex, the fully myelinated white matter is prominently T1-hyperintense (left) and T2-hypointense (right). Again, there are no subcortical temporal cysts. The third row (C) shows the MRI of patient 3 at 11 years. This patient has a de novo heterozygous c.528_530dup, p.(Ala177dup) variant in *GPRC5B*. The sagittal T1-weighted image (left) and axial FLAIR image (middle) reveal bilateral anterior temporal subcortical cysts (red arrows). The axial T2-weighted image (right) shows prominent hyperintensity and swelling of the cerebral white matter, leading to broadened gyri. This MRI is indicative of classic MLC. The fourth row (D) demonstrates the MRI in patient 4, the boy with a homozygous c.643G>A, p.(Ala215Thr) *AQP4* variant, at 8 months of age. The sagittal T1-weighted (left) and axial FLAIR (middle) images reveal bilateral anterior temporal subcortical cysts. The axial T2-weighted image (right) shows hyperintensity and slight swelling of especially the subcortical cerebral white matter. The fifth row (E) illustrates the major improvement on follow-up of the same boy at 4 years. The anterior temporal subcortical cysts have become smaller (left and middle) and the cerebral white matter is mostly normal (right). Pt, patient; m, months; y, years

Figure 2 The Ala215Thr variant disrupts membrane localization of AQP4 in stably transfected MDCK cells. (**A**) Schematic illustration of AQP4 structure.[37] Transmembrane domains (1-6) and intracellular and extracellular loops (A-E) are indicated. NPA motifs in loop B and E assemble in the membrane to form a crucial part of the channel pore. The amino acid substitution observed in patients (Ala215Thr) localizes to the second NPA motif. (**B**) Western blot analysis of MDCK cells after stable transfection with wild-type AQP4 shows presence of the

protein. In contrast, no protein is detected in five different MDCK lines stably transfected with AQP4 Ala215Thr, suggesting immediate degradation of the mutant protein. See Supplementary Fig. 2 for full-length blots. (**C**) Cell surface biotinylation experiments on MDCK cell lines show complete absence of membrane AQP4 Ala215Thr (AQP4 surface expression normalized to wild-type: wild-type AQP4: 1.00±0.20, *n*=4; Ala215Thr AQP4: 1: 0.00±0.01, *n*=4; 2: 0.02±0.05, *n*=4; 3: 0.01±0.01, *n*=4; 4: 0.06±0.08, *n*=4; 5: 0.07±0.02, *n*=4). (**D**, **E**) Representative traces of cell volume changes in MDCK cell lines upon exposure to a hypertonic shock (injection of a mannitol solution) to induce cell shrinking (D) and hypotonic shock (injection of distilled water) to induce cell swelling (E), measured using calcein-quenching.[14] Fluorescence is normalized to baseline, and corrected for fluid-injection artefacts. (**F**, **G**) Calculation of shrinking/swelling rate constants for different MDCK cell lines shows that stable transfection of wild-type AQP4 (black) significantly increases rate constants when compared to non-transfected (empty) MDCK cells (grey). In contrast, rate constants for all five AQP4 Ala215Thr lines (blue) are indistinguishable from empty MDCK cells. Shrinkage rate constant (s^{-1}): empty: 0.072±0.007, *n*=4; wild-type AQP4: 0.800±0.031, *n*=4; Ala215Thr AQP4: 1: 0.079±0.006, *n*=4; 2: 0.082±0.005, n=4; 3: 0.081±0.003, n=4; 4: 0.062±0.008; 5: 0.081±0.005, n=4). Swelling rate constant (s^{-1}): empty: 0.115±0.004, *n*=4; wild-type AQP4: 0.676±0.035, *n*=4; Ala215Thr AQP4: 1: 0.102±0.006, *n*=4; 2: 0.098±0.004, n=4; 3: 0.096±0.007, n=4; 4: 0.083±0.011; 5: 0.096±0.007, n=4). Data are presented as mean ± SEM.

Figure 3 The Ala215Thr variant in AQP4 disrupts membrane localization and channel function. (**A**) Confocal imaging of HEK293T cells overexpressing GFP tagged wild-type or Ala215Thr AQP4 (green). Wild-type AQP4 co-localizes with a fluorescent membrane marker (WGA; magenta), indicating membrane expression. Membrane expression is strongly reduced for Ala215Thr AQP4. (**B**) Magenta and green fluorescence intensity profiles along dotted lines drawn in (A). (**C**) Wild-type AQP4 shows significantly more membrane localization than Ala215Thr AQP4 (membrane/cytosol fluorescence ratio: wild-type AQP4: 2.68±0.61, *n*=26; Ala215Thr AQP4: 0.38±0.05, *n*=21; $P<0.001$). Mean cytosolic fluorescence does not significantly differ between wild-type and Ala215Thr AQP4 transfected cells (not shown). (**D**) SDS-page followed by western blot mainly shows monomeric and dimeric AQP4 in cells transfected with wild-type AQP4, while Ala215Thr AQP4 mostly forms protein aggregates. See

Supplementary Fig. 3 for full-length blots. (**E**) Cell surface biotinylation reveals strongly reduced membrane expression for Ala215Thr when normalized to wild-type (normalized AQP4 surface expression: 0.40±0.07, *n*=3, *P*=0.029). (**F**) Left, cell volume changes in transfected HEK293T cells upon exposure to a 40% hypotonic or hypertonic shock, measured using calcein-quenching. Fluorescence changes are normalized to those measured in non-transfected cells. Therefore, normalized fluorescence changes indicate transfection mediated changes in cell volume dynamics (see supplementary methods for details). Wild-type AQP4 expressing cells shown in black, Ala215Thr AQP4 expressing cells in blue. (**G**) Quantification of the speed of cell volume changes. Wild-type AQP4 expressing cells rapidly change volume upon osmotic challenge, reflected by a higher slope of the swelling/shrinking phase (black). Ala215Thr AQP4 expressing cells show significantly slower changes in cell volume (blue; shrinking speed ($F*s^{-1}$): wild-type -0.0056±0.0006, *n*=23 versus Ala215Thr -0.0033±0.0003, *n*=18, *P*=0.003; swelling speed ($F*s^{-1}$): wild-type 0.0083±0.0013, *n*=13 versus Ala215Thr 0.0005±0.0002, *n*=11, *P*<0.001). Data are presented as mean ± SEM.

Figure 4 GPRC5B localization in the human brain. (**A-C**) Representative immunofluorescence images from human frontal white matter sections, stained for the astrocyte protein GFAP (magenta, A), the nuclear staining DAPI (blue), the endothelial cell marker CD31 (magenta, B), the MLC-related protein GlialCAM (magenta, C) and GPRC5B (green). GPRC5B is present in astrocyte somata (A), and additionally shows a clear vascular / perivascular staining (B,C). Perivascular GPRC5B is surrounded by, but not fully overlapping with, GlialCAM staining. (**D, E**) Example immunofluorescence images from grey matter, showing localization of GPRC5B to the glia limitans (D), and its absence in neuronal cell bodies (as stained with NeuN, magenta, E). (**F**) Example image from the subventricular zone, showing GPRC5B expression in ependymal cells lining the ventricles. (**G**) Electron microscopy images from human frontal white matter, showing immunogold labelling for GPRC5B in different cell types surrounding blood vessels. lc: lymphocyte; ac: astrocyte; ec: endothelial cell; pc: pericyte; ax: axon. Magenta arrows indicate membrane associated GPRC5B staining, blue arrows indicate intracellular GPRC5B staining. Scale bars: 50 µm for A-F; 1 µm for G.

Figure 5 GPRC5B variants alter regulatory volume decrease, and GPRC5B modulates VRAC. (**A**) GPRC5B schematic, highlighting duplicated amino acids in the 4th transmembrane segment (red). (**B**) RVD measurements in lymphoblasts exposed to a hypotonic shock. Averaged cell surface dynamics for 5 control lymphoblast lines (black) and 3 GPRC5B patient lines (orange). (**C**) RVD percentage in lymphoblasts. Points indicate individual cells, bars represent average ± SEM per cell line, dotted lines indicate mean RVD for all control (black) and all GPRC5B patient (orange) lines. Patient cells show reduced RVD (controls: 60.1±3.4%, *n*=103 cells from 5 subjects versus patients 44.4±3.4%, *n*=100 cells from 3 subjects, *P*=0.001). (**D**) Western blot for GPRC5B, MLC1 and TRPV4 (β-Actin as loading control) on 3 control and 3 GPRC5B patient lymphoblast cell lines. Molecular weight markers on the left. See Supplementary Fig. 4 for full-length blots. (**E**) Densitometric analysis of protein bands normalized to β-Actin (2-4 replicate experiments). Patient cells show increased GPRC5B levels (controls: 10.0±2.8, patients: 23.0±1.4, *P*=0.003), but unaltered MLC1 levels (controls: 16.7±0.5, patients: 16.7±0.8, *P*=0.95). TRPV4 levels were reduced (controls: 25.8±4.5, patients: 9.2±1.4, *P*=0.005). (**F**) Representative patch-clamp current traces under isotonic and hypotonic conditions in a non-transfected (empty; left) and a wild-type GPRC5B (isoform 1) transfected U251 cell (right). Traces in response to voltage steps (-100 mV to +100mV). Scale bars: 200 ms (x), 1 nA (y). (**G**) Averaged I/V relationship of hypotonically activated VRAC current density in empty, wild-type GPRC5B, Ala177dup GPRC5B, and Ile176dup GPRC5B expressing U251 cells. (**H**) Averaged VRAC current density at +100 mV in U251 cells. Overexpression of all GPRC5B variants of both isoforms significantly increased VRAC current (empty: 14.9±4.3 pA/pF, *n*=15, isoform 1 wild-type: 60.0±10.3 pA/pF, *n*=12, *P*=0.01; isoform 1 Ala177dup: 52.0±9.2 pA/pF, *n*=17, *P*=0.02; isoform 1 Ile176dup: 67.9±11.5 pA/pF, *n*=16, *P*=0.001; isoform 2 wild-type: 89.5±17.6, *n*=12, *P*<0.001; isoform 2 Ala177dup: 57.4±13.3, *n*=15, *P*=0.03; isoform 2 Ile176dup: 55.9±12.4, *n*=15, *P*=0.04). No significant differences between Ala177dup, Ile176dup and wild-type GPRC5B were found (*P*-values >0.99). (**I**) VRAC current density in MLC1-overexpressing U251 cells. GPRC5B overexpression (isoform 1) has no additional effect on MLC1 overexpression-augmented VRAC activation (empty: 53.0±17.5 pA/pF, *n*=8, wild-type: 49.7±16.5 pA/pF, *n*=6, *P*>0.99; Ala177dup: 60.6±19.2 pA/pF, *n*=5, *P*>0.99; Ile176dup: 54.0±19.6 pA/pF, *n*=4, *P*>0.99). Also, no significant differences between Ala177dup and

Ile176dup GPRC5B variants and wild-type GPRC5B were found (P>0.99). All data presented as mean ± SEM.

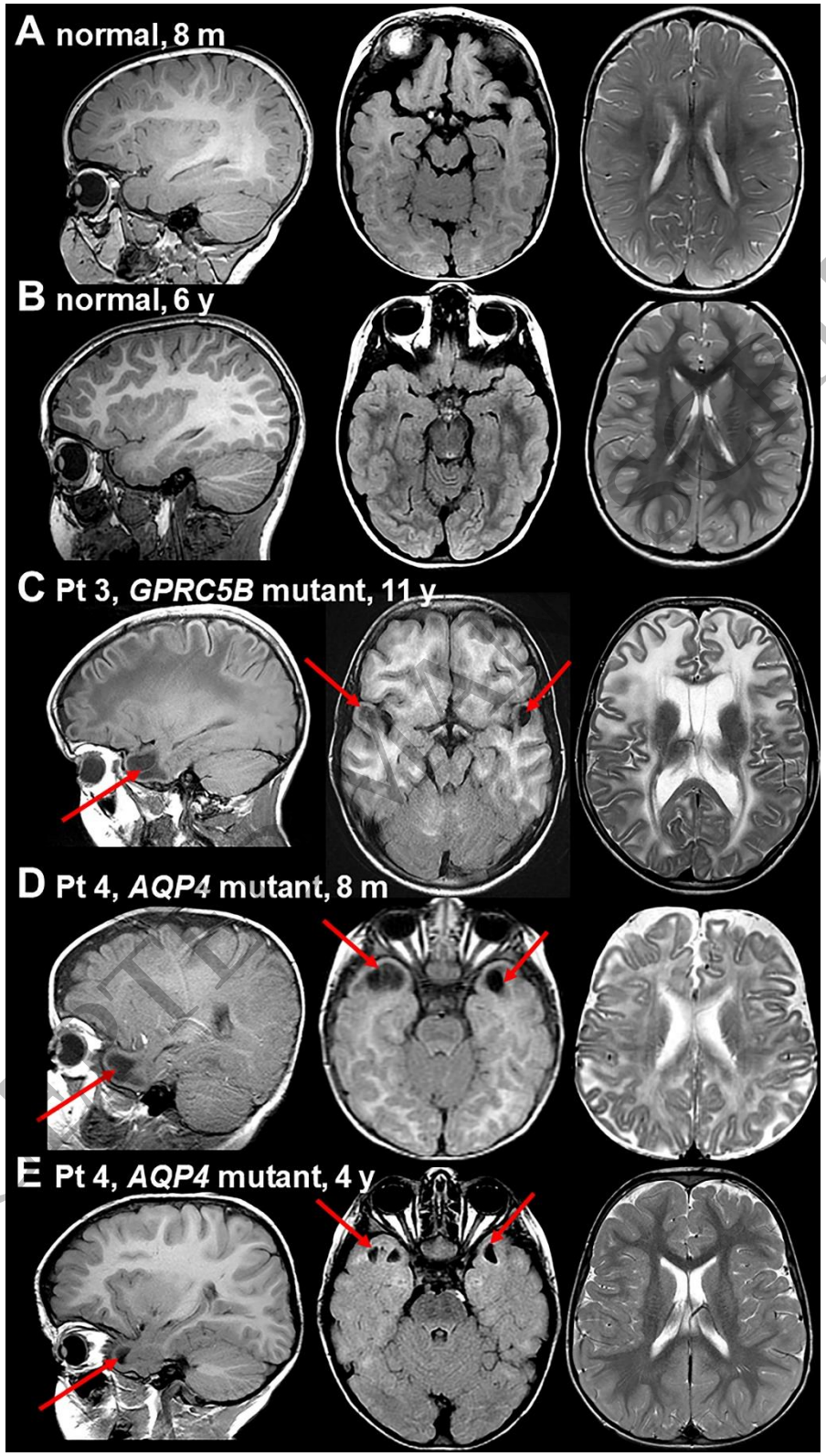

Figure 1
190x339 mm (x DPI)

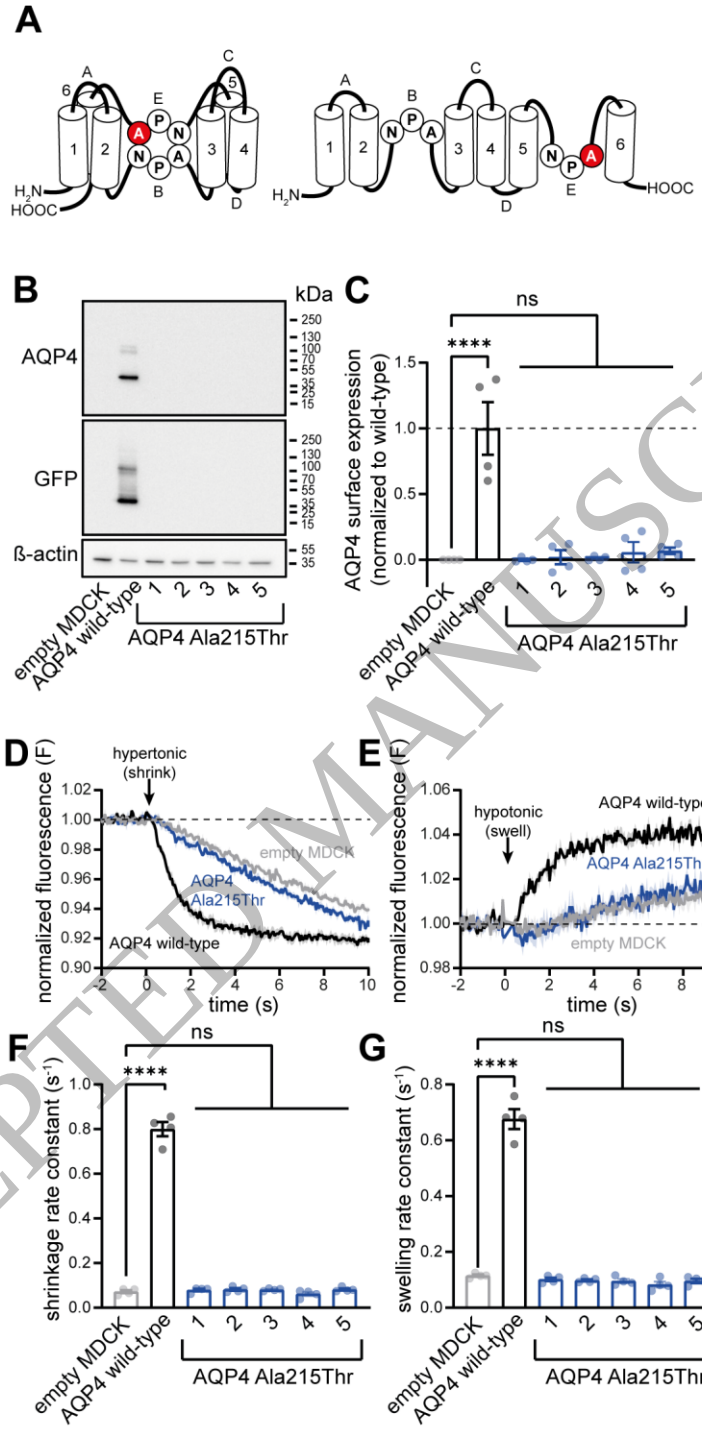

Figure 2
102x193 mm (x DPI)

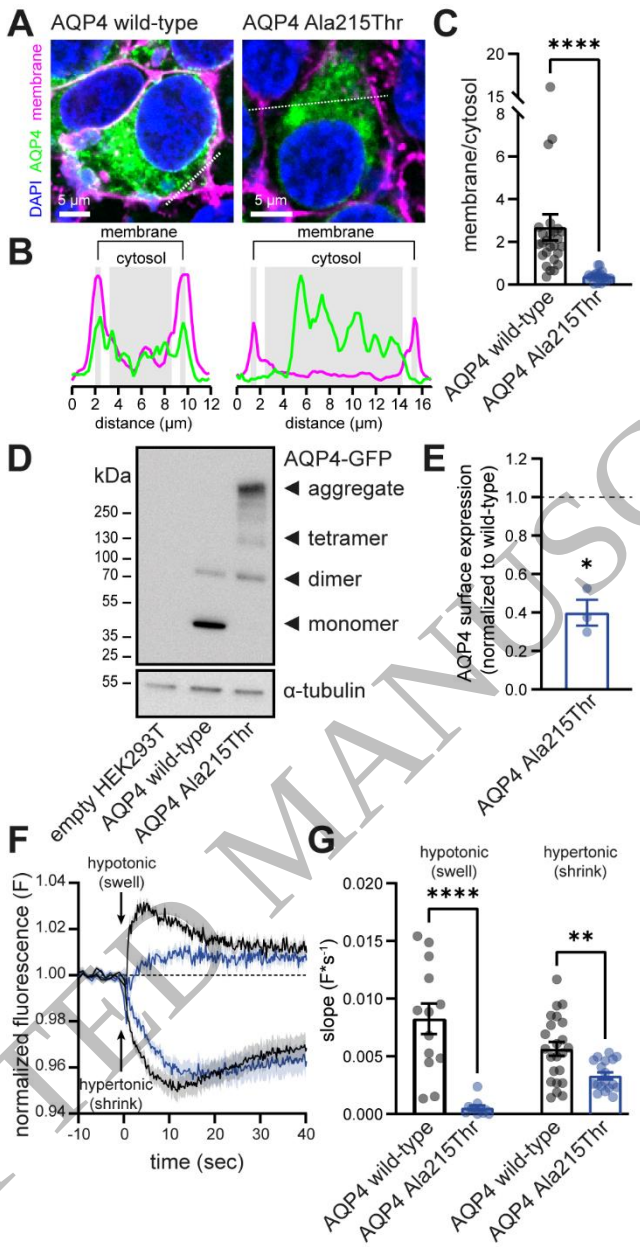

Figure 3
83x164 mm (x DPI)

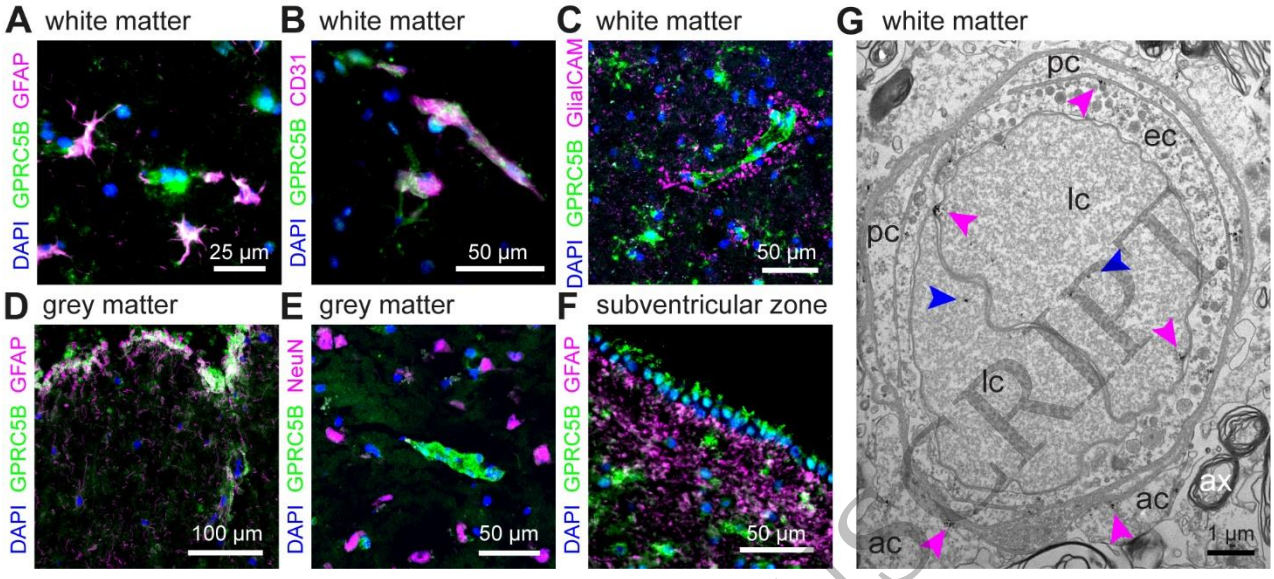

Figure 4
168x75 mm (x DPI)

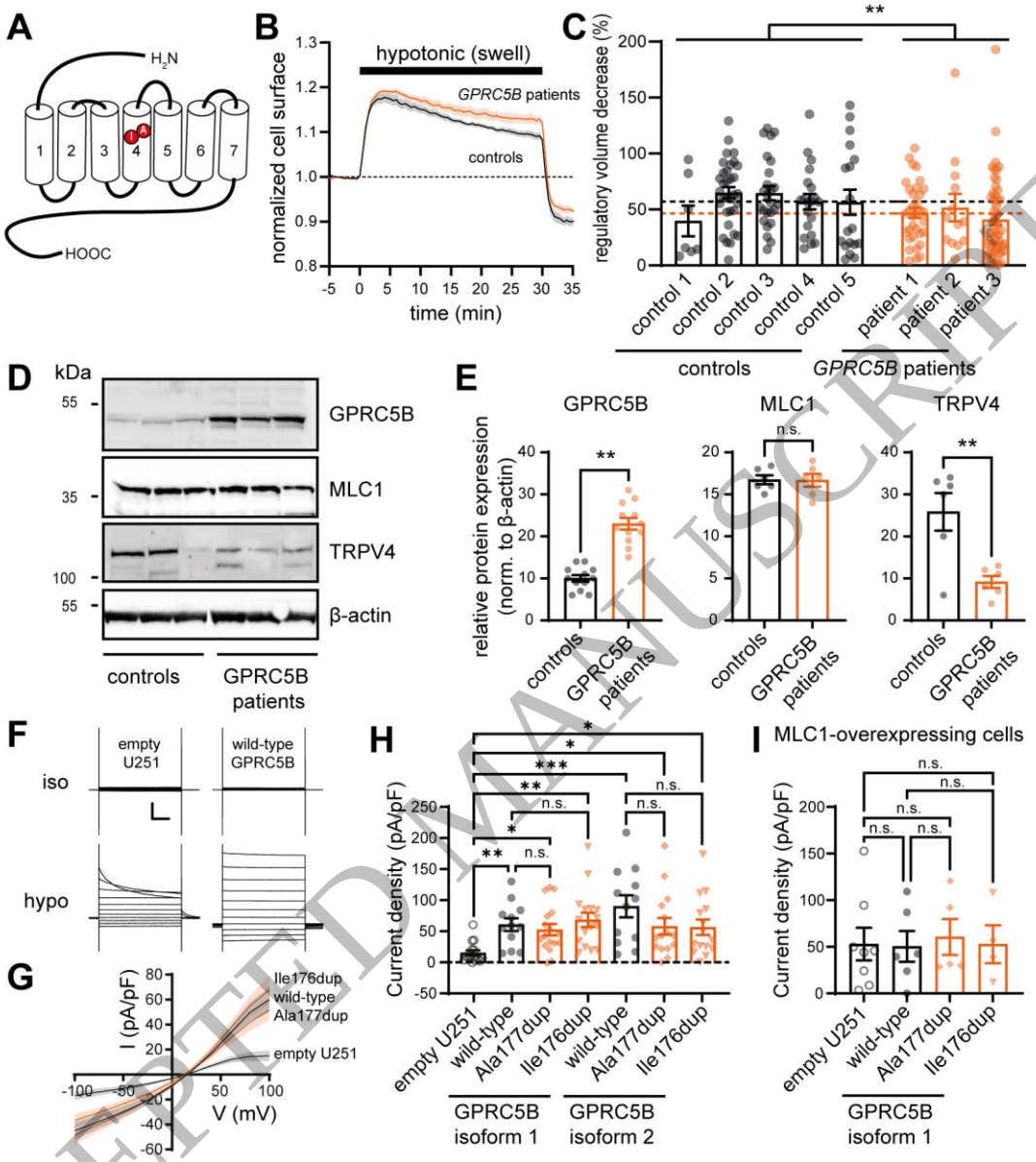

Figure 5
141x159 mm (x DPI)